



Symmetry: A guide to its application in 2D electron crystallography

Michael J. Landsberg ^{*}, Ben Hankamer ^{*}

Institute for Molecular Bioscience, Queensland Biosciences Precinct, The University of Queensland, Brisbane, Qld 4072, Australia

Received 1 May 2007; received in revised form 19 June 2007; accepted 6 July 2007

Abstract

A defining property of a crystal is its symmetry. This mini-review sets out to summarize all aspects that define 2D crystallographic symmetry as applied to the study of macromolecular structure. It begins by defining molecular point symmetries, before covering crystallographic symmetry operations in 2D, common notation, a summary of crystallographic plane groups and theoretical methods and important considerations for the identification and application of symmetry in 2D crystal images for 3D structure determination. While many of the concepts covered here may be equally applicable to point symmetry and space group symmetry in 3D, this review has been written from the perspective of 2D electron crystallography and deals specifically with symmetry operations and crystallographic space groups in 2D crystal projection images.

Crown copyright © 2007 Published by Elsevier Inc. All rights reserved.

Keywords: Crystallographic symmetry; Plane group; 2D space group; Point symmetry; 2D electron crystallography

1. Introduction

Symmetry is a property which exists in objects and structures as diverse as natural and synthetic materials, mathematical equations and musical compositions. At a broad, fundamental level, symmetry implies that an object can be rearranged in some way without changing its appearance. Spatially, this can be thought of as a manipulation imposed on the object (e.g. rotation) leading to some interchange of points in space, but which results in an arrangement which is indistinguishable from the original. Such manipulations are termed *symmetry operations*.

All symmetry operations require a point, axis, or plane of reference, about which they are applied. This reference is termed the *symmetry element* (e.g. axis of rotational symmetry, plane of mirror symmetry) and is characterized by the fact that points lying on the element, remain unchanged following the symmetry operation. The above definitions suggest that many objects contain several symmetry elements, all of which can be applied individually or in com-

ination. Indeed this is the case, and it follows that for such objects this “set” of all symmetry operations adheres to the rules of a mathematical group. The set of all symmetry operations applicable to the object is therefore referred to as the *symmetry group* of the object.

Structural biology benefits greatly from the presence and correct identification of symmetry, which is often present in 2D and 3D crystals as well as multi-subunit macromolecular assemblies—true symmetry in the strictest sense does not exist as every molecule is different due to, for example, conformational flexibility and molecular thermal motion, however, where the overall assembly is close enough to a given symmetry, its imposition is justified. This allows accurate, averaging of symmetry-related data-points in 3D space and in turn greatly assists in the determination and refinement of 3D structure. A basic example is the averaging of each half of a homo-dimer with the other to increase the quality of the final reconstruction.

This review summarizes the relevance of symmetry to the analysis of two-dimensional (2D) crystals by covering crystallographic symmetry operations in 2D, common notation, a summary of all the 2D space groups, and theoretical methods and important considerations for the identification and imposition of symmetry in 2D crystal images.

^{*} Corresponding authors. Fax: +61 7 33462101.

E-mail addresses: m.landsberg@imb.uq.edu.au (M.J. Landsberg), b.hankamer@imb.uq.edu.au (B. Hankamer).

While many of the concepts covered here may be equally applicable to point symmetry and space group symmetry in 3D, this review has been written from the perspective of 2D electron crystallography and will deal specifically with symmetry operations and crystallographic space groups in 2D.

2. Molecular symmetry

Molecular structures are often defined in terms of the *point group* that they belong to, or alternately as having particular *point symmetry*. The term point symmetry derives from that fact that a point symmetry operation is one which leaves at least one point in space unmoved (Bernal et al., 1972; Glazer, 1987).

In general terms, point symmetry usually comes in one of five flavors; cyclic, dihedral, tetragonal, octahedral (or cubic) and icosahedral. The simplest of these are the *cyclic* point groups, having one axis of n -fold rotational symmetry, where n is an integer greater than 1 (Fig. 1A). Theoretically, n has no maximum however some of the highest cyclic point groups observed for proteins to date are seen in the structures of the bacteriophage SPP1 portal protein, gp6 (C_{13} symmetry) (Orlova et al., 1999), a chloroplast ATP synthase (C_{14} symmetry) (Seelert et al., 2000) whilst larger structures such as the *S. typhimurium* type III secretion needle (19- to 22-fold) (Marlovits et al., 2004) and the *S. enterica* M-ring (24- to 26-fold) and C-ring (32- to 36-fold) flagellar rotor components (Thomas et al., 2006) are known to have higher but variable symmetry.

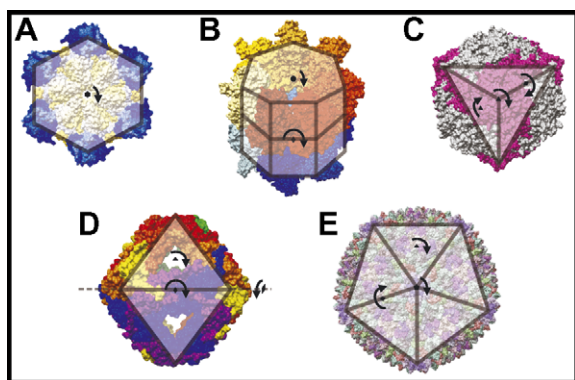


Fig. 1. Point symmetry in molecular structures. (A) The p97 ATPase (Zhang et al., 2000) (PDB ID = 1E32) has C_6 symmetry. (B) GroEL (Ranson et al., 2001) (PDB ID = 2C7E) has D_7 symmetry. (C) Insect ferritin (Hamburger et al., 2005) (PDB ID = 1Z6O) differs from other ferritins in that it has tetrahedral symmetry. (D) The Hsp16.5 complex (Kim et al., 1998) (PDB ID = 1SHS) has octahedral or cubic symmetry. (E) The viral capsid of bacteriophage PRD1 (Abrescia et al., 2004) (PDB ID = 1W8X) is an example of icosahedral symmetry. In each example, the regular polyhedron defining the symmetry of the molecule is superimposed on the structure. Rotation axes are indicated by arrows, with the length of the arrow corresponding to the order of rotational symmetry (i.e. 6-fold rotation symmetry indicated by an arrow demonstrating a one-sixth turn). In the octahedral example, the 4-fold axis (---) is orthogonal to the direction of view. Structures are not to scale.

Dihedral point groups, like the corresponding C_n structure, have a similar axis of n -fold rotational symmetry, but additionally have a 2-fold rotation axis orthogonal to the main axis of rotation (i.e. two, C_n rings stacked on top of one another, with equivalent surfaces of the ring in contact, would typically generate the corresponding D_n point group; Fig. 1B).

Tetragonal structures such as insect ferritin (Hamburger et al., 2005) belong to the same symmetry group as a regular tetrahedron and contain 12 copies of the asymmetric unit (Fig. 1C). Specifically, they have two distinct sets of 3-fold rotation axes (four copies of each; $4 \times 3 = 12$) and six 2-fold axes ($6 \times 2 = 12$) and are thus often referred to as having 3–2 symmetry. Structures with *cubic* or *octahedral* symmetry such as the Hsp16.5 small heat shock protein from *M. Jannaschii* (Kim et al., 1998) have six 4-fold rotation axes, eight 3-fold rotation axes and twelve 2-fold (4–3–2 symmetry) and are thus 24-fold symmetric (Fig. 1D).

Many viruses assemble into structures with *icosahedral* symmetry (Caspar and Klug, 1962) with some of the best characterized examples including Rice Dwarf, Semliki Forest, bacteriophage PRD1 and Hepatitis B viruses (Abrescia et al., 2004; Bottcher et al., 1997; Mancini et al., 2000; Zhou et al., 2001). These have the same symmetry as a regular icosahedron or dodecahedron and feature twelve 5-fold rotation axes, twenty 3-fold rotation axes and thirty 2-folds, hence icosahedral structures are often referred to as having 5–3–2 symmetry and contain 60 copies of the asymmetric unit (Fig. 1E).

3. Crystallographic symmetry

The fundamentals of molecular point symmetry introduced above form the basis for a fuller explanation of crystallographic symmetry. Protein crystals (2D and 3D) are essentially a regularly arrayed lattice of molecular structures, however, some point symmetry operations are forbidden in crystal symmetry. Additionally, crystals often belong to a different symmetry group compared with the point group of the molecular building block (Schenk et al., 2005; Vonck et al., 2002). By calculating all permutations arising from the combination of each allowed crystallographic symmetry operation (rotation, mirror, glide, screw, roto-inversion), we arrive at a finite number of symmetry groups (*crystallographic space groups*) which collectively describe all possible crystallographic packing arrangements. A total of 230 space groups define all possible crystallographic packing arrangements. Consequently, any 3D crystal will conform to the symmetry rules of at least one of these groups. For protein crystals, only 65 of these space groups are possible. The other 165 space groups contain mirror symmetry, forbidden in protein crystals because all naturally occurring amino acids are chiral molecules with “L” stereochemistry; the mirrored molecule having “D” stereochemistry does not naturally occur. Electron crystallographers typically work with so-called “2D” crystals, which are usually no more than one to two mole-

cules thick. Projection images of 2D crystals can be described by the symmetry rules of at least one of the 17 *plane groups* (so named because they occupy a single plane in 3D space, by convention the *xy* plane).

3.1. Crystal parameters

All crystals can be built from a minimum, asymmetric, repeating motif (the *asymmetric unit*). It contains no internal symmetry and therefore cannot be generated by the application of a symmetry operation to some subset of the points it is composed of (Fig. 2). The asymmetric unit of a crystal can also be the unit cell, but quite often it is not. The *unit cell* is effectively a tile within a repeated pattern—it must be possible to generate the crystal solely by placing several thousand copies of the unit cell together end to end, with no spaces or gaps (Fig. 2). Importantly, this can only be achieved by translating the unit cell along a vector exactly equal in magnitude to the unit cell length in the direction of translation. No other manipulation of the unit cell is permitted—a crystal which breaks this rule indicates that the unit cell has been incorrectly defined. Put more succinctly, a unit cell is generated by the imposition of point symmetry operations on the asymmetric unit, while the imposition of translation symmetry operations on the unit cell generates a *crystal lattice*.

3.2. Unit cells

The unit cell is defined as the smallest area exhibiting the full point symmetry of the crystal. The unit cell of a 2D crystal is often characterized by four parameters—the *plane group* describing its symmetry as well as the physical dimensions of the cell, vectors termed *a* and *b* (crystallographic convention denotes that *b* is horizontal and *a*

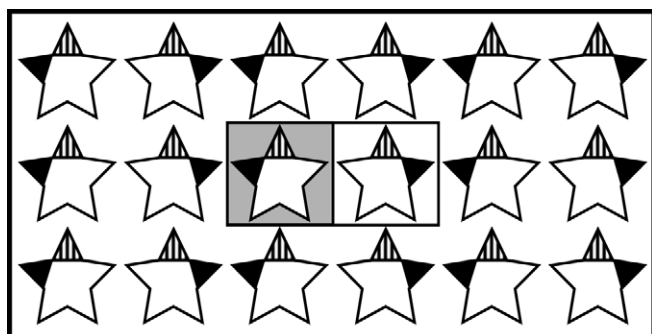


Fig. 2. Building blocks of a 2D crystal. A single star (bordered by grey shading) represents the asymmetric unit of this pattern. It is impossible to entirely reproduce the pattern shown by mere translation of one star. To do so requires generation of a second “crystallographically related” star, the mirror image of the first. This mirror symmetry operation generates the unit cell (outlined by rectangular black border). The “crystallographic dimer” of stars can then be tiled along a vector equivalent in magnitude to the length of the unit cell in the direction of translation to generate the pattern or “crystal” as shown.

points downward), and the angle between these, γ (by convention $180 \geq \gamma \geq 90$) (Glaeser, 2007). Four unit cell geometries are possible in 2D crystals, rhomboid ($a \neq b$, $\gamma > 90$), rectangle ($a \neq b$, $\gamma = 90$), square ($a = b$, $\gamma = 90$) or rhombus ($a = b$, $\gamma = 120$).

The unit cell of a 2D crystal can be either a primitive or a centered cell. A *primitive cell* is the minimum, translationally repeated unit cell contained within the crystal, or to describe this another way, encompasses a single lattice point of the crystal. In some cases, however, the unit cell of the crystal may contain more than one lattice point. With respect to 2D crystals, unit cells of this type are referred to as *face-centered*. The term derives from the fact that the cell is equivalent to a single face of the 3D unit cell described by the same term, however in 2D the “face” prefix is redundant as it is physically impossible for the unit cell of a 2D crystal to be centered anywhere other than on the face of the 3D space group from which it derives.

An excellent example of the difference between a primitive and centered cell is seen in the monomeric porin OmpG which crystallizes in at least two forms (Behlau et al., 2001). In the first crystal form, the protein packs such that a single lattice point consists of four crystallographically related porin molecules (Fig. 3A). This motif can be translated periodically in both dimensions to reproduce the crystal and therefore is a primitive unit cell. In the second crystal form the lattice point consists of a crystallographic dimer (Fig. 3B). Closer examination of the crystal packing arrangement however reveals that the dimer is incorporated into a pseudo-hexagonal packing arrangement. This crystal packing arrangement can be reproduced from a primitive unit cell by choosing an oblique cell (shown in red), however this unit cell does not contain mirror symmetry. A centered unit cell (shown in green), containing multiple copies of the dimer, does however reproduce the full crystal packing arrangement and in addition, contains mirror symmetry. The centered cell is therefore chosen to describe the space group of this molecule as it is the simplest unit cell which describes the full symmetry of the crystal. Of the 17 possible 2D space groups, 15 are primitive cells with the remaining two being centered cells (Table 1).

4. Point symmetry operations

The *crystallographic point group* of a 2D crystal essentially describes symmetry operations involving *rotation* of the unit cell about an axis (or point in the projection image), or generation of a *mirror* image about a plane (or line). As will be explained below, there are a total of 10 crystal point groups in 2D (Table 1, column 4), nine of which derive from all possible combinations of these two symmetry operations in addition to the point group, *I*, which describes crystals with no point symmetry.

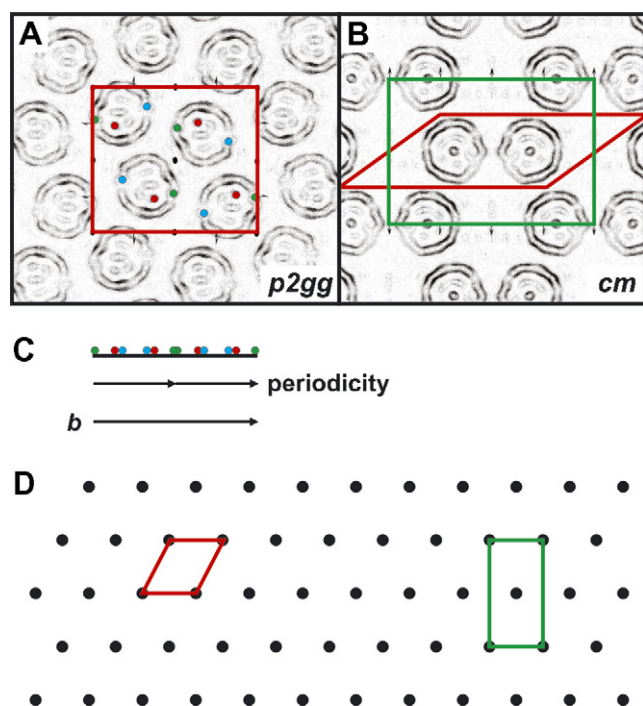


Fig. 3. Primitive and centered cells. The monomeric porin OmpG crystallizes in at least two forms (Behlau et al., 2001). (A) The $p2gg$ form is described by a primitive unit cell (red box). Symmetry-related structural features have been highlighted with colored circles for the purpose of identifying the periodicity in C. (B) A centered cell (green) is required to describe the symmetry of the cm crystal form in its entirety. An alternate primitive cell is outlined in red which describes the minimum, translationally repeated motif but this cell does not describe the full symmetry of the crystal (i.e. it lacks a mirror plane). (A) and (B) adapted from Behlau et al. (2001). (C) The structural information in (A) has been reduced to a 1D function coincident with one of the screw axes present in the crystal. Note that the crystal has internal repetition along this axis with a periodicity of $b/2$. (D) Primitive cells (red) are the smallest unit cell required to describe the minimum repeating motif of the crystal, while centered cells (green) encompass multiple lattice points and thus have internal repetition.

4.1. Rotation symmetry

Crystal images with rotation symmetry are typically termed n -fold rotationally symmetric, or as having a rotation axis of order n . This implies that rotation of the image by $360/n^\circ$ results in a new orientation which is indistinguishable from the original. The symmetry element associated with rotation is strictly an axis, however in 2D crystal images the axis is orthogonal to the image plane and so rotation in 2D effectively occurs about a point in the image.

While molecular assemblies can theoretically have rotation axes of infinite order, crystallographic structures are restricted to having rotation symmetry of order 2, 3, 4 or 6. This derives from theories first put forward by R.-J. Haüy as early as the turn of the nineteenth century (see Senechal (1990)), who hypothesized that the basic building blocks of crystals could be grouped into plane shapes that filled space (Fig. 4). This theory severely limits the geome-

try of the fundamental building blocks of a crystal, in that only a rhomboid and the regular triangle, square and hexagon efficiently fill space (i.e. can be arrayed infinitely with no gaps or spaces). Note that these polygons exhibit 2, 3, 4 and 6-fold symmetry, respectively, and define the allowed orders of rotational symmetry within crystal space groups. The crystal restriction theorem, readily found in many crystallography texts, further highlights this fact by essentially stating that it is impossible to build a lattice with 5-fold rotation symmetry, or any rotational symmetry of order seven or higher. Importantly, this does not prohibit a 5-fold symmetric assembly from crystallizing, but rather prohibits the formation of a 5-fold symmetric crystal lattice.

Rotation symmetry alone defines four of the 10 possible 2D crystal point groups: 2, 3, 4 and 6 are the 2D point groups which contain a rotation axis of order 2, 3, 4 or 6, respectively. Rotation symmetry alone, however, does not describe the point groups of all symmetric objects and assemblies in nature. Additional crystallographic point groups derive from the existence of mirror symmetry in the projection of a structure.

4.2. Mirror symmetry

As mentioned previously, mirror symmetry is forbidden in individual protein structures. However, it is important to realize that 2D crystal images used in electron crystallography can exhibit mirror symmetry. The key difference between 2D crystals and their TEM projection images is that in the latter, the true molecular 3D structure of the 2D crystal is compressed into a single plane (xy by convention). The result of this is an inability to discern structural information relative to the z -axis and in the case of 2D crystals specifically, an apparent loss of chirality in images projected orthogonal to the plane of crystallization. Thus, while true mirrors in 3D protein structures are not possible, mirrors in untilted 2D projection images are (Fig. 5). Ultimately, the 3D information can be recovered (with the exception of the ‘missing cone’) by tilting specimens, but it is important to remember that a single micrograph considered independent of any other contains no discernible information orthogonal to the projected plane.

In an image with mirror symmetry (often referred to as reflection symmetry) all points equidistant from, and along a line orthogonal to the symmetry element are equivalent. In 3D space, the mirror operation occurs about a plane. In 2D, the mirror plane is always orthogonal to the image plane, so the mirror element in 2D is therefore a line (or axis). Mirrors are often said to give rise to 2-fold symmetry as they yield two copies of the asymmetric unit.

Unlike rotational symmetry, which can generate multiple point groups depending on the order of rotation (i.e. 2, 3, 4 and 6; recall 1 is no symmetry), a unit cell either has or does not have mirror symmetry. Therefore, a unit cell containing a single mirror element and no other symmetry belongs to the point group m . The remaining 2D

Table 1
The 17 2D space groups

Plane group ^a	Unit cell geometry (Crystal system ^b)	Rotation order	Point symmetry	Glide	2D space group ^{d,e}
<i>p1</i>	Rhomboid (Oblique)	1	1	N	P1
<i>p2</i>	Rhomboid (Oblique)	2	2	N	P2
<i>pm</i>	Rectangle	1	<i>m</i>	N	P12
<i>pg</i>	Rectangle	1	<i>m</i>	Y	P12 ₁
<i>cm</i>	Rectangle	1	<i>m</i>	N	C12
<i>p2mm</i>	Rectangle	2	<i>2mm</i>	N	P222
<i>p2mg</i>	Rectangle	2	<i>2mm</i>	Y	P222 ₁
<i>p2gg</i>	Rectangle	2	<i>2mm</i>	Y	P22 ₁ 2 ₁
<i>c2mm</i>	Rectangle	2	<i>2mm</i>	N	C222
<i>p4</i>	Square	4	4	N	P4
<i>p4mm</i>	Square	4	<i>4mm</i>	N	P422
<i>p4gm</i>	Square	4	<i>4mm</i>	Y	P42 ₁ 2
<i>p3</i>	Rhombus ^c (Hexagonal)	3	3	N	P3
<i>p3m1</i>	Rhombus ^c (Hexagonal)	3	<i>3m</i>	N	P321
<i>p31m</i>	Rhombus ^c (Hexagonal)	3	<i>3m</i>	N	P312
<i>p6</i>	Rhombus ^c (Hexagonal)	6	6	N	P6
<i>p6mm</i>	Rhombus ^c (Hexagonal)	6	<i>6mm</i>	N	P622

^a Hermann–Mauguin or International notation. Describes the symmetry of 2D projection images.

^b Indicated if different from the unit cell geometry.

^c Denotes rhombus with an internal angle of 60°.

^d Describes the space group of 2D crystals (Holser, 1958) and gives rise to the plane group indicated in column 1 when projected at 0° tilt.

^e The output from the MRC program ALLSPACE conforms to this notation with the exception that subscripted numerals appear as standard font in the output.

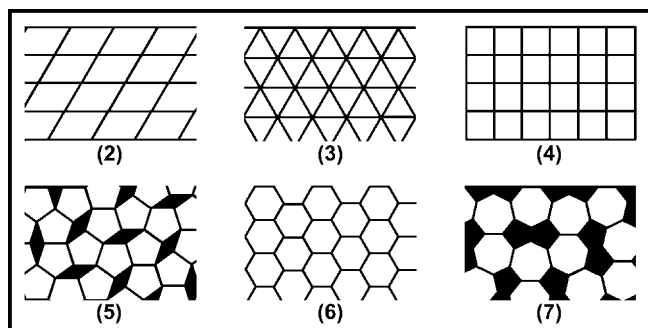


Fig. 4. Rotational symmetries compatible with crystal packing. Only unit cells with rotational symmetry of order two, three, four or six can efficiently fill a single plane (no black space). These correspond to the only allowed crystallographic symmetries. Regular polygons with either 5-fold or 7-fold symmetry and above do not efficiently fill space (black space). Adapted from Senechal (1990).

point groups (*2mm*, *3m*, *4mm* and *6mm*) derive from combinations of each order of rotation symmetry with mirror symmetry, where a second *m* indicates that the symmetry of the point group generates an additional mirror plane orthogonal to the first.

5. Translation operations

Crystals differ from symmetric molecules and macromolecular assemblies in that they contain additional symmetry operations beyond those described by their point group. This stems from the fact that they are a repeated array built from the unit cell. The *plane group* of a 2D crystal describes

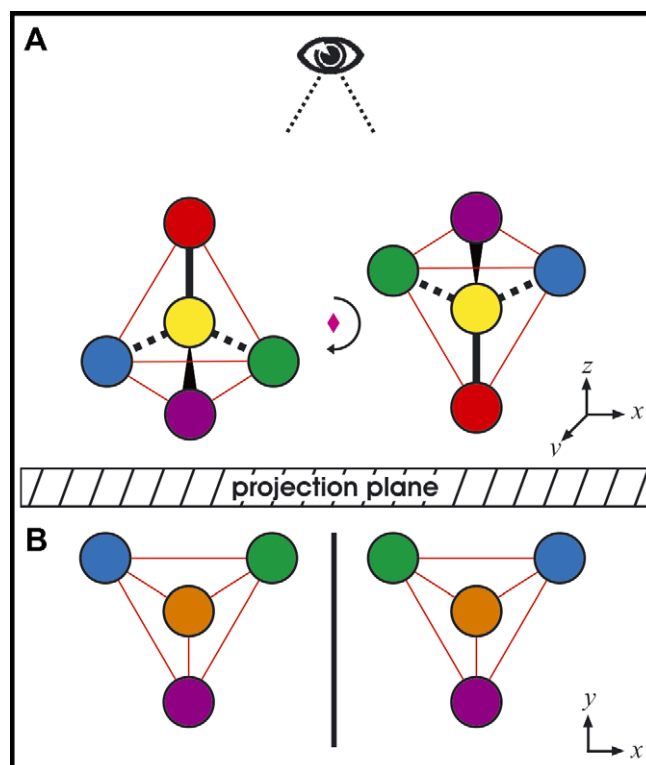


Fig. 5. Mirror symmetry in 2D projection space. (A) 3D representations of two identical chiral molecules with the same stereochemistry. One is rotated 180° relative to the other. Projection of the 3D molecules in (A) from the position of the eye onto the projection plane generates the projection images shown in (B). Note that in these images, the relative depth of the atoms along the *z*-axis can no longer be distinguished. Note also that the two projection images are mirror images despite the fact they derive from identical, chiral molecules.

two types of symmetry, these being the point group symmetry of the crystal as well as any additional symmetry operations involving translation. Unlike point symmetry operations, translation operations do not leave any points in space unmoved. All 2D crystals have two translational symmetry operations along the unit cell vectors a and b . Additionally, translation is often combined with other symmetry operations (i.e. mirrors, rotation) to generate more complex symmetry operations (i.e. glide, screw).

5.1. Glides and screws

Several symmetry operations restricted to 3D space can occur in 2D crystals, as they are (thin) 3D objects. For example, simple 2-fold rotation of asymmetric units about an axis parallel to the crystallization plane yields mirror symmetry in the projection image of a crystal (Fig. 5). This reinforces the reason why mirrors are observed in 2D crystal images.

More complex symmetry operations also take place in 3D space. The only operation applicable to biological molecules, however, is the *screw operation*. A screw operation occurs about an axis (the general notation is an n_p screw axis) and combines translation along the axis by a fraction of the unit cell, p/n , followed by right-handed, n -fold rotation about the same axis. For example, a 2_1 screw axis ($n = 2$, $p = 1$) describes a translation of $1/2$ (p/n) of the unit cell followed by rotation of 180° ($360/n$) about the axis of translation.

A screw operation is essentially a special application of rotational symmetry and its degree of rotation is restricted in the same way as a simple axis of rotation. Given that p must be an integer value less than n , it follows that the possible screw axis operations are limited to 2_1 , 3_1 , 3_2 , 4_1 , 4_2 , 4_3 , 6_1 , 6_2 , 6_3 , 6_4 and 6_5 . The 3_2 , 4_3 , 6_4 and 6_5 operations are often referred to as enantiomorphous operations, as they are essentially left handed equivalents of the 3_1 , 4_1 , 6_2 and 6_1 screw operations, respectively.

2D crystals can, and often do, contain screw axes parallel to the plane of crystallization. The 2_1 screw axis is particularly prevalent in 2D membrane protein crystals and in fact is the only screw axis observed in crystals of this nature. The reasons for this are both spatial in that the crystal thickness restricts the screw axis to the xy plane (theoretically, screw axes orthogonal to the membrane plane are not forbidden, but to date, none have been reported), and steric—the positioning of the hydrophobic transmembrane region of the protein within the lipid bilayer usually means it is only possible for the protein to insert in the membrane in either an “up” or “down” orientation (for examples see Heymann et al. (2003); Levy et al. (1999)). This means that the rotation operation will always occur through 180° .

Recall that rotation of an object by 180° about an axis within the 2D plane of the crystal results in a mirror plane in the projection image of the crystal (Fig. 5). It thus follows that a 2_1 screw axis is manifested in a projection image

as a translation by $1/2$ of a unit cell, followed by a mirror operation about the translation vector. This type of symmetry operation is termed a *glide* (the element is a glide plane) and generates four further crystallographic space groups in 2D; the m , $4mm$ and $2mm$ point groups all give rise to plane groups which can contain glide symmetry, the latter accommodating glide axes in two different arrangements.

6. Crystallographic notation in 2D

6.1. Projection images and plane group notation

Towards the end of the nineteenth century, Fedorov, Schönflies and Barlow independently enumerated the crystallographic space groups which result from all possible combinations of the crystallographically allowed symmetry operations (see Blundell and Johnson (1976)). In 2D, there are 17 possible space groups (wallpaper groups or referred to herein as plane groups), at least one of which will serve to describe any possible 2D crystal form. Of these, 16 have been identified by the concepts described thus far—the 10 pure point symmetry space groups ($p1$, $p2$, $p3$, $p4$, $p6$, pm , $p2mm$, $p3m$, $p4mm$, $p6mm$), the additional four space groups which arise from a subset of these by the imposition of glide symmetry (pg , $p2mg$, $p2gg$, $p4gm$), and a further two centered-cell space groups (cm , $c2mm$). The final space group arises from the fact that the $3m$ point group generates two space groups, depending on the location of the mirror plane ($p3m1$, $p31m$). These 17 2D plane groups are summarized in Table 1.

Plane groups are most commonly defined using the Hermann–Mauguin or International notation. As can be seen in Table 1, this notation represents each plane group by a maximum of four characters. The first, either p or c , indicates a primitive or centered unit cell. The second is a digit (1 , 2 , 3 , 4 or 6) indicating the highest order of rotational symmetry in the crystal. Note that for some space groups with no rotational symmetry, the 1 is omitted. Note further that only the highest rotational symmetry is indicated. For example, the $p4$ space group also has a 2-fold rotation axis. This is implied and does not need to be explicitly stated in the space group definition.

The third and fourth characters indicate additional symmetry(s) and their position(s) relative to the main axis of translation (i.e. the unit cell vector b). There are three options here; an m indicates a mirror plane, a g indicates a glide axis and a l (if present) indicates no symmetry. The third character indicates a symmetry axis orthogonal to the main axis of translation (b). The fourth character indicates a symmetry axis either parallel to (for $n = 2$; where n is the rotational symmetry of the plane group) or rotated $180^\circ/n$ (for $n > 2$) relative to the main axis of translation. The two space groups belonging to $3m$ point symmetry can now be delineated; $p3m1$ has a mirror plane rotated 90° relative to the unit cell vector b , while $p31m$ has a similar symmetry plane 60° rotated from b .

A full description of the symmetry rules for the 17 crystallographic plane groups is given in the International Tables for Crystallography (Hahn, 2002). By way of example, images of 2D crystals of the RC47 reaction center of photosystem II (Rhee et al., 1997) demonstrate the symmetry operations defining the space group $p2gg$. The unit cell has a rotation axis of order two (Fig. 6A, S1). In addition, the crystal contains glide symmetry in two directions. The first glide axis is positioned orthogonal to main axis of translation (unit cell vector b ; Fig. 6B, S2), while the second is parallel to b (Fig. 6C, S3). This crystal therefore conforms to the rules of space group $p2gg$ and contains all the symmetry elements described by it.

6.2. Space group notation for 2D crystals

At this point, it is important to make a distinction between the space group assigned to a 2D crystal projection image and the space group of a 2D crystal. Projection

images of 2D crystals can be described by one of the 17 plane groups outlined above and referred to by the Hermann–Mauguin notation. The 2D crystal itself though is described by a different space group. As mentioned previously, 2D crystals are truly 3D in nature and symmetry operations such as mirrors and glides, while allowed in 2D crystal projection images, are forbidden in 2D crystals of proteins. Similarly, screws and rotation axes in the plane of the crystal are possible in 2D crystals but are not present in plane group definitions.

Fortunately, the notation used to describe the space group of a 2D crystal (Table 1, column 6) maps somewhat trivially to the Hermann–Mauguin notation used to describe the plane group of untilted crystal projection images (Amos et al., 1982). The characters used to indicate a primitive or centered cell remain the same (P or C), however it is conventional to indicate the type of unit cell of a 2D space group using a capital letter rather than the lower case notation used for the plane groups. Mirror planes

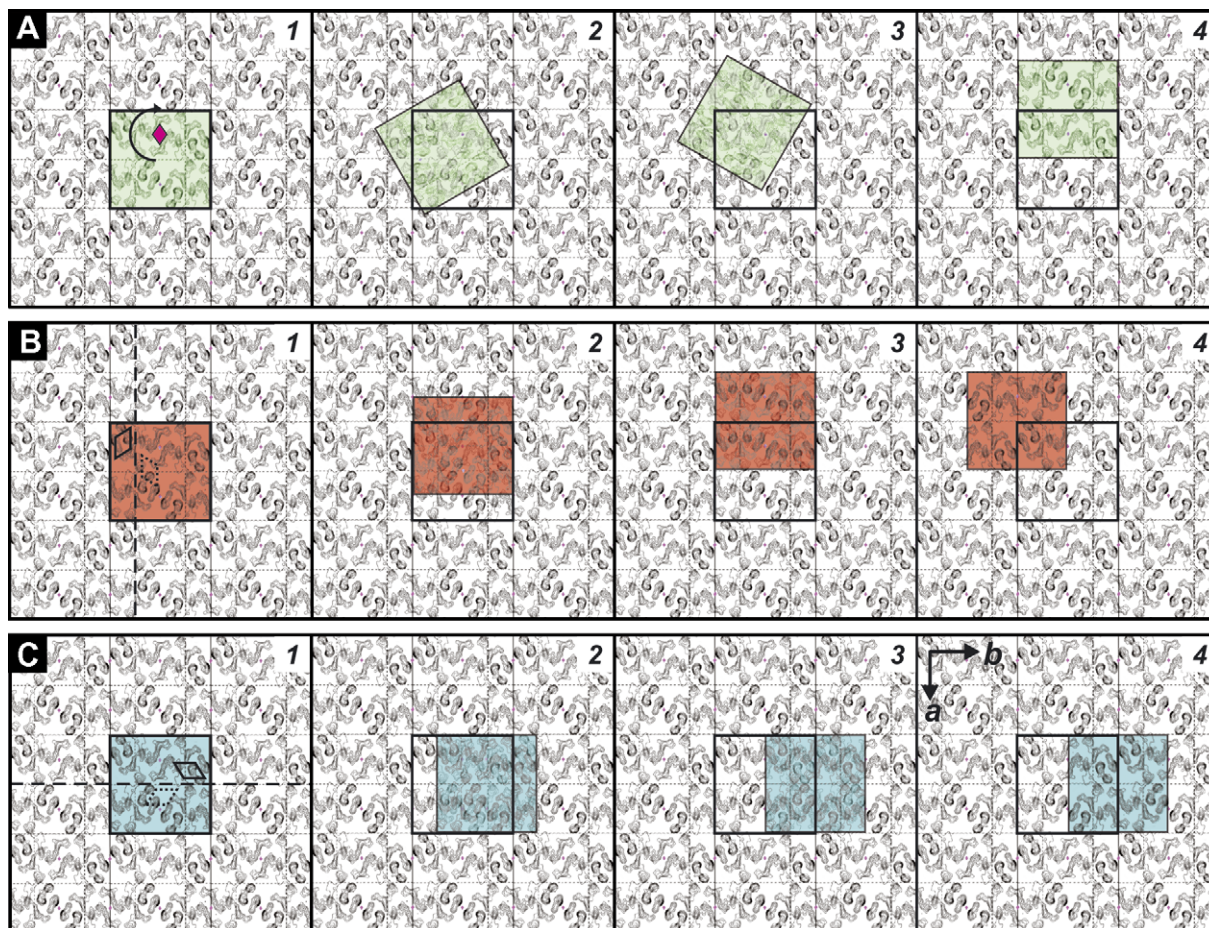


Fig. 6. Symmetry operations of the space group $p2gg$. Crystals of the photosystem II RC47 reaction center belong to the space group $p2gg$ (Rhee et al., 1997). Each row indicates a different symmetry operation and each column within the row shows selected steps of an animation which illustrates the symmetry operation. (A) A 2-fold rotation axis is positioned orthogonal to the plane of the page at the center of the magenta diamond. Frames 2, 3 and 4 illustrate the rotation. (B) A glide axis is indicated by the vertical dashed line. The unit cell is translated in the direction of this axis by half a unit cell (frames 2 and 3) and then reflected about the element (frame 4). (C) A second glide axis is indicated by the horizontal dashed line with subsequent frames as indicated for B. Note that in frame 4 of all panels, the unit cell superimposes perfectly on the structural information in the target area of the image, indicating that the symmetry operation generates symmetrically related structures. Adapted from Rhee et al. (1997). Movies are available as Supplementary material.

(indicated by m in plane groups) are replaced by a 2 subsequent to the order of rotation symmetry. This derives from the fact that, as shown earlier, mirror symmetry in a projection image arises from the presence of a 2-fold axis of rotation within the plane of crystallization. In the same manner, glide planes (indicated by a g in plane groups) are replaced by a 2_1 which indicates a 2_1 screw axis. Thus by way of example, the space group of a 2D crystal, the untilted projection image of which belongs to plane group $p2mm$, is denoted $P222$. Similarly, a 2D crystal projection image belonging to plane group $p2gg$ derives from a 2D crystal belonging to space group $P22_12_1$.

7. Symmetry and image processing

7.1. Image processing in Fourier space

The Fourier transform of a crystal describes its structure in reciprocal space and is non-zero only at a regular array of points, often referred to as diffraction spots. Diffraction spots lie on a periodic lattice defined by the basis vectors a^* and b^* , the magnitudes of which are inversely proportional to the respective real space vectors a and b , and can be derived from the general formula for a 3D unit cell, given in (Blundell and Johnson, 1976) as

$$a^* = \frac{Kbc \sin \alpha}{V}; \quad b^* = \frac{Kca \sin \beta}{V}$$

where $V = abc\{1 + 2\cos\alpha\cos\beta\cos\gamma - \cos^2\alpha - \cos^2\beta - \cos^2\gamma\}^{1/2}$.

Given that in the case of a 2D crystal c is by convention orthogonal to the ab plane, it follows that the angles α and β are always 90° and the formulae thus reduce to

$$a^* = \frac{K}{a\sqrt{1 - \cos^2\gamma}}; \quad b^* = \frac{K}{b\sqrt{1 - \cos^2\gamma}}$$

where K is a constant and the included angle, γ^* , is given by $(180 - \gamma)$.

By determining the reciprocal lattice vectors of a crystal, it is subsequently possible to identify the coordinates of each reciprocal lattice point (diffraction spot) within the crystal Fourier transform. Given that all structural information pertaining to the crystal is sampled at these lattice positions, it is then possible to eliminate a large fraction of the background noise from 2D crystal images by masking out the diffraction spots in Fourier space (Fourier filtration).

Lattice points are often described in terms of a $(h k)$ coordinate system, where h and k are integer multiples of the reciprocal lattice vectors a^* and b^* , respectively. For example, the position of the (21) reflection is located by the vector sum $2a^* + b^*$. In 3D, a third coordinate, l , is used to describe the reciprocal lattice in the third dimension, however 2D crystals exhibit no lattice in 3D and the Fourier transform of a 2D crystal is in fact a continuous function in the direction of the z^* axis. In images of untilted specimens—the only images from which symmetry can be accurately determined— l (or alternatively, z^*) always

equals 0. Thus for simplicity, coordinates are only referred to here in the format $(h k)$.

7.2. Crystallographic symmetry in Fourier space

Real space and Fourier space representations of data are intrinsically linked, such that any symmetry present in real space crystal images must also be preserved in Fourier space. This important property can be derived from first principles, and is significant at two levels of electron crystallographic image processing. First, the space group of a crystal can be reliably determined through the identification of symmetry within the Fourier transform of the crystal. Second, once the space group of a crystal is known, a better estimate of the true structural information described by the transform can be obtained by Fourier averaging of symmetry-related data points identified by the symmetry rules of the crystallographic space group.

At a first pass, potential crystal symmetries can be narrowed down using the shape of the diffraction pattern, or more specifically the values of a^* , b^* and γ^* . For example, a crystal with 4-fold rotation symmetry will have a square unit cell, meaning that γ approximates to 90° and $a \approx b$. As a further example, a crystal having 6-fold rotation symmetry will always exhibit hexagonal packing, meaning the unit cell will have a value of approximately 120° for γ . This in turn means that $\gamma^* \approx 60^\circ$, so the $p6$ and $p6mm$ unit cell in real space will always have a hexagonal lattice in Fourier space, with the first order reflections (01) , (10) , $(1-1)$, $(0-1)$, (-10) and (-11) positioned at the vertices of a regular hexagon. Unfortunately, this will not distinguish between a $p6$ and a $p6mm$ crystal. Nor will it distinguish the three space groups with 3-fold rotational symmetry, as these also exhibit a hexagonal lattice (due to the existence of Friedel pairs in Fourier space).

Investigation of the unit cell parameters can therefore assist in narrowing down the possible space groups of a crystal, but in practice it is necessary to compare the actual phase and amplitude measurements at each lattice point to fully elucidate the space group of a crystal. Systematic absences, if present, can also give clues as to the space group of a crystal.

7.3. Systematic absences

Another useful tool for evaluating the space group of a 2D crystal is the identification of systematic absences within a crystal Fourier transform. Systematic absences are the result of *symmetry forbidden reflections*, a phenomenon which results from periodicity within the crystal occurring over less than a full unit cell. Such periodicity occurs where glide or screw symmetry is present in the crystal or where a centered cell has been chosen to describe the crystal. Axial or zonal systematic absences arise from screws and glides, respectively, and in 2D, for example, cause the systematic absence of all odd reflections along

Table 2
Symmetry-forbidden reflections in 2D space groups

Projection symmetry	Crystal symmetry	Real space glide parallel to	Systematic absences ($n = \text{any integer}$)
<i>pg</i>	P12 ₁	<i>b</i>	(0 <i>k</i>): $k = 2n + 1$
<i>cm</i>	C12	—	(<i>h k</i>): $h + k = 2n + 1$
<i>p2mg</i>	P222 ₁	<i>a</i>	(<i>h</i> 0): $h = 2n + 1$
<i>p2gg</i>	P22 ₁ 2 ₁	<i>a, b</i>	(0 <i>k</i>): $k = 2n + 1$ (<i>h</i> 0): $h = 2n + 1$
<i>c2mm</i>	C222	—	(<i>h k</i>): $h + k = 2n + 1$
<i>p4gm</i>	P42 ₁ 2	<i>a, b</i>	(0 <i>k</i>): $k = 2n + 1$ (<i>h</i> 0): $h = 2n + 1$

b^* (where the glide is parallel to real space vector b). When the structural information is condensed into a 1D function along a single vector coincident with the screw axis, it can be seen that the pattern repeats with a periodicity equal to half the unit cell ($b/2$; see Fig. 3C). Translated into reciprocal space, this means the true periodicity of the lattice becomes $2b^*$ and hence every odd reflection along b^* becomes symmetry forbidden.

Choosing a centered cell to describe a crystal leads to what are known as integral systematic absences. Due to the fact that a centered cell encompasses two lattice points (causing internal repetition; Fig. 3D) the centered cell generates twice as many theoretical reflections as the alternate primitive cell of the same crystal. Half of the reflections generated by the centered cell are therefore symmetry forbidden. A summary of the systematic absences expected for the five 2D plane groups in which they occur is given in Table 2.

7.4. Phase comparisons

Friedel's law states that the diffraction spots ($h k$) and ($-h -k$) have equal intensities (or amplitudes) and opposite phases. Above and beyond this relationship, the introduction of symmetry dictates that lattice points related by symmetry (not necessarily Friedel pairs, for example, in $p3$) have theoretically identical amplitudes and phases. This provides the basis for rules allowing for the space group of a crystal to be unequivocally assigned based purely upon a list of amplitude and phase measurements at each lattice point in the Fourier transform.

Perhaps the most commonly used software for symmetry evaluation in electron crystallography is the ALLSPACE routine (Valpuesta et al., 1994) within the MRC (Crowther et al., 1996) and 2DX (Gipson et al., 2007) image processing packages, the latter of which uses a modified version of the original MRC program. ALLSPACE evaluates the data in a crystal Fourier transform and attempts to assign a space group to the crystal based on a table of phase comparisons (phase measurements are usually more accurate than image-derived amplitudes owing to the effects of factors such as the contrast transfer function, specimen charging and drift, on image contrast). In this way, *phase residuals* (the difference between measured phases and theoretical or average values) are often used to identify the quality

of the fit of crystallographic data to the rules of a particular space group and are also used to assess the quality of data used to resolve a structure.

Consider the case of a crystal belonging to plane group $p2$. In this example, the corresponding Fourier transform must also have 2-fold rotation symmetry. This means that not only must the amplitudes of any diffraction spot be the same as the spot to which it is directly opposite (i.e. when rotated 180° about the origin) but their phases must also be equal.

Taking this a step further, consider the true nature of a Fourier transform of a 2D projection as being essentially a 2D frequency space representation of a series of waves (cosine functions) which reconstruct the real space image. For an image with 2-fold rotation symmetry, these cosine waves must therefore also be symmetric about the real space phase origin. To satisfy this, the peak or trough of the cosine wave must be positioned at the origin (corresponding to a phase shift of 0° or 180° , respectively; Fig. 7). Such space groups, referred to as centrosymmetric, are therefore easily detected by the observation that all phases approximate to either 0° or 180° (provided the data have been shifted to their appropriate real space origin). This holds true not only for the space groups with rotation

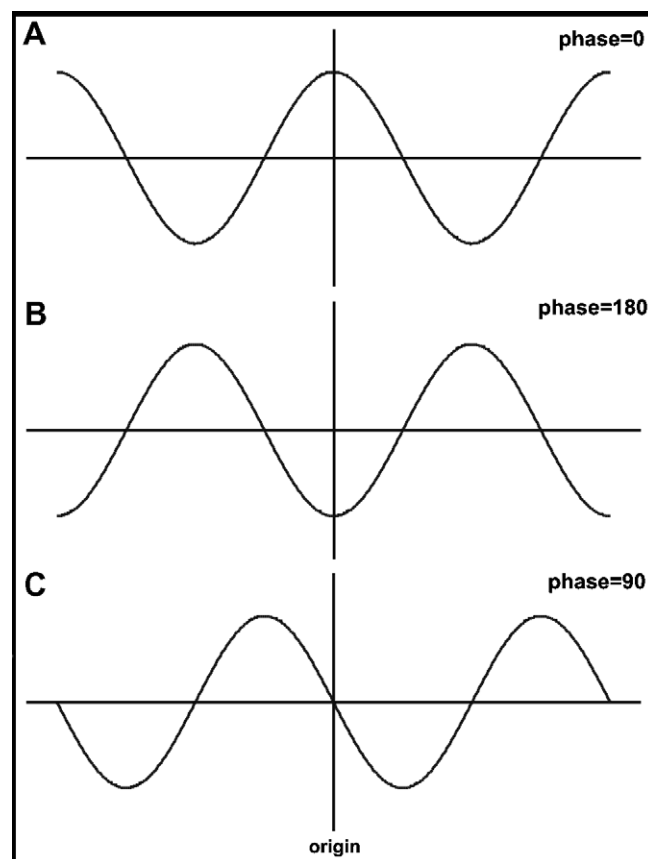


Fig. 7. Centrosymmetric space groups have a requirement that all phases must equal 0° or 180° . This is because the cosine function must be symmetric about the real space phase origin, and this is only possible when the phase of the cosine wave is 0° (A) or 180° (B). If the wave is displaced by any other amount relative to the origin (as shown in (C) for 90°) the symmetry is lost.

axes of order two ($p2$, $p2mm$, $p2mg$, $p2gg$, $c2mm$), but also for all higher order space groups which have inherent 2-fold rotational symmetry (i.e. all space groups with 4-fold or 6-fold rotation symmetry; $p4$, $p4mm$, $p4gm$, $p6$, $p6mm$; Fig. 8).

The identification of symmetry in Fourier space can be extended to all symmetry operations. For a crystal with inherent 3-fold rotation symmetry (i.e. $p3$, $p3m1$, $p31m$, $p6$ and $p6mm$ space groups), the reflections related by a 120° rotation about the origin (e.g. the first order reflections (10) (0 -1) and (-11)) have theoretically identical phases. It follows that the presence of $p3$, $p3m1$ and $p31m$ symmetry can be differentiated from $p6$ and $p6mm$ as the latter will also adopt phases of 0° and 180° as they are centrosymmetric. By extension of this theory, the $p4$, $p4mm$ and $p4gm$ space groups are characterized by the presence of inherent 2-fold symmetry as outlined above, along with the additional restraint that rotation by 90° will yield identical phases (e.g. the (11), (-1 -1), (-1 1) and (1 -1) reflections will all be identical; Fig. 8).

Similarly, where mirror symmetry is present in the real space projection image of a crystal, there is also mirror

symmetry in the Fourier transform. Diffraction spots equidistant from and along a line orthogonal to the mirror plane of the Fourier transform are expected to have identical phases (Fig. 8). If a glide plane is present, the same spots are related as in mirror symmetry, with the difference being that the screw causes a phase shift of 180° (Fig. 8).

For plane groups with a single mirror or glide plane, the position of the symmetry element is important in identifying symmetry-related reflections. For example, by convention the mirror plane of a pm unit cell is located parallel to b . In Fourier space, this translates to the (11) and (-1 1) reflections being related by symmetry. If a^* and b^* are incorrectly identified or interchanged (which frequently occurs, for example, when a and b have comparable magnitudes) this symmetry rule no longer holds. However, the (11) and (1 -1) now become symmetry-related, as the mirror plane is merely mislocated relative to the reciprocal lattice vectors. ALLSPACE therefore searches 21 plane group definitions in order to accommodate the four plane groups (pm , pg , cm , $p2mg$) for which the positions of glide or mirror planes relative to unit cell vectors are important. This means it is possible to detect the presence of symmetry in a crystal, even if the diffraction pattern has been indexed incorrectly.

By using the rules summarized above for the detection of rotation, mirror and glide symmetry it is possible in the majority of cases to identify unequivocally the plane group of a 2D crystal based purely on a table of phase comparisons. Where the plane group is not immediately clear, it is sometimes possible to differentiate between alternative plane groups by combining these rules with information on systematic absences. Importantly, only the modified programs in 2DX version 2.1 and later consider systematic absences when assigning a space group, however due consideration should be given to the fact that systematic absences can be broken under certain conditions (e.g. relatively thick specimens, negative stain). By way of comparison, the original ALLSPACE relies on the fact that amplitude and phase measurements at the coordinates of symmetry forbidden reflections have a very low signal-to-noise ratio and are therefore drastically down weighted when converting diffraction data to a 3D model or 2D projection map.

8. Considerations for symmetrical averaging of data

The preceding sections of this review have discussed several key concepts pertaining to the symmetry of 2D crystals and ways of identifying symmetry in 2D crystal projection images. It is important to note however that these symmetry rules are easily broken if a number of assumptions regarding the data in question are not met.

While 2D projection images contain the full 3D information of the specimen, they do not delineate this information along the z -axis. It is normal to acquire images of tilted specimens in order to recover this 3D information, however plane group symmetry rules will only remain valid for the analysis of untilted specimen images. This stems from the

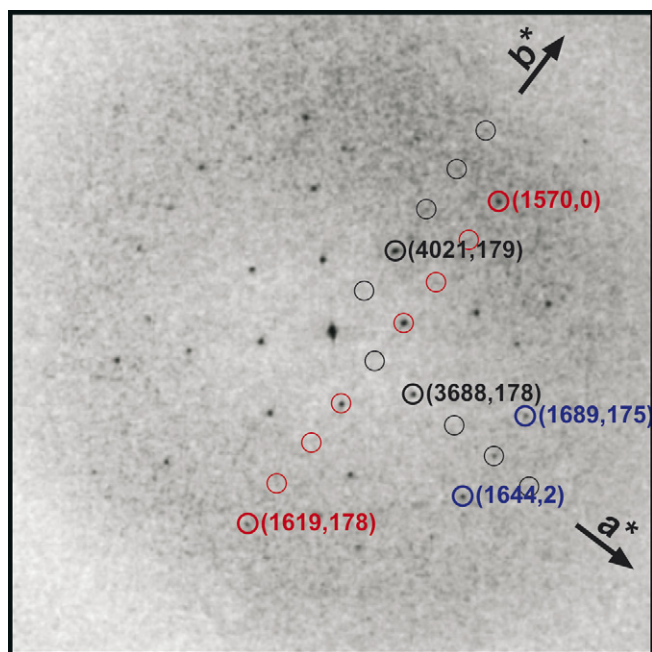


Fig. 8. Symmetry in Fourier space. Crystals of CHIP28/AQP-1 belong to plane group $p4gm$ (Mitra et al., 1994). Amplitude and phase data are listed in parentheses next to the corresponding bold circled spot. The (20) and (02) reflections (black) are related by 4-fold rotation symmetry and mirror symmetry and therefore have near identical phases (the mirror axes in $p4gm$ bisect the lattice vectors). The glide axes in $p4gm$ lie parallel to the unit cell vectors, meaning the (14) and (1 -4) reflections should theoretically be out of phase by 180° (red), as are the (41) and (4 -1) reflections (blue). Additionally, (14) and (4 -1) are related by 4-fold rotation symmetry, as are (41) and (1 -4). Note that the phase measurements of symmetry-related spots are significantly more precise than the amplitude measurements. Note also that this space group is centrosymmetric, meaning all phases approximate to 0° or 180° . Adapted from Mitra et al. (1994).

fact that upon tilting a specimen, diffraction spots that were previously related by symmetry now sample different values in z^* (in fact, approximately inverse values, depending on the resolution and curvature of Ewald's sphere) and therefore are no longer identical. Crystal tilts of as little as 2° can completely abolish symmetry (Unger et al., 1997), particularly in thick specimens. It is thus imperative that the space group of a crystal is determined from crystal images with 0° tilt.

Equally important is the assumption that images used for space group determination do not exhibit any significant astigmatism. For a non-astigmatic image, the effect of the CTF is uniform at equivalent distances from the origin, and since symmetry-related reflections are themselves equidistant from the origin, they are all affected by the CTF uniformly (i.e. what was the same in Fourier space prior to being multiplied by the CTF, remains the same afterwards). When astigmatism is introduced this clearly is no longer the case. Astigmatism distorts the CTF into an ellipsoid meaning that the modulation of amplitude data by the CTF at symmetry-related lattice points is no longer uniform.

The plane group symmetry rules of a crystal only ever hold when the crystal unit cell is centered relative to the plane group it belongs to, i.e. the data must be shifted to the crystallographic phase origin. ALLSPACE achieves this by systematically shifting the unit cell data in both directions and testing the symmetry at each location. In this way, it is possible to identify the putative plane group of a crystal and the corresponding phase origin at the same time.

For negatively stained specimens, symmetry detection can often be adversely influenced by the contribution of symmetry artifacts resulting from the stain exclusion pattern. This usually results in over-estimation of the crystal symmetry (Unger, 2000) and for this reason, it is often suggested that the plane group of a crystal is independently confirmed (i.e. from a vitrified specimen) prior to imposing higher order symmetries in particular. Symmetry artifacts may also be revealed by sub-symmetries not being identified by symmetry detection programs (i.e. the absence of $p3$ symmetry from a proposed $p6$ crystal would suggest the $p6$ symmetry is an artifact).

Finally, when merging data it is important to check the symmetry of each dataset, ensuring only the lowest detected symmetry is imposed on the merged data. For example, whilst projection symmetry is lost in tilted specimens, most 2D space groups impose other constraints along certain lattice lines in 3D. Such verification is important in identifying rare cases where the 2D space group of a crystal may not be the same as what is suggested from the plane group of untilted projections. It is also important to verify symmetry when moving to progressively higher resolution as macromolecular assemblies frequently have higher apparent symmetry at low resolution. For example, the insect ferritin structure in Fig. 1 appears to have cubic symmetry at low resolution, however at higher resolution,

the differences between the heavy and light chains of this hetero-oligomer become apparent and the symmetry reduces to tetrahedral.

9. Concluding remarks

This mini-review provides an in depth summary of the key concepts relating to electron crystallographic symmetry. In particular it aims to provide structural biologists new to the field of electron crystallography with a solid basis allowing for the accurate identification of symmetry and the subsequent application of symmetry based averaging in structure refinement. Furthermore, it provides a summary of useful information for more advanced users.

Acknowledgments

We thank R. Glaeser for helpful discussions and advice on the manuscript. We also thank D. Woolford, H. Stahlberg and V. Unger for further helpful discussions.

Appendix A. Supplementary data

Supplementary data associated with this article can be found, in the online version, at [doi:10.1016/j.jsb.2007.07.002](https://doi.org/10.1016/j.jsb.2007.07.002).

References

- Abrescia, N.G., Cockburn, J.J., Grimes, J.M., Sutton, G.C., Diprose, J.M., Butcher, S.J., Fuller, S.D., San Martin, C., Burnett, R.M., Stuart, D.I., Bamford, D.H., Bamford, J.K., 2004. Insights into assembly from structural analysis of bacteriophage PRD1. *Nature* 432, 68–74.
- Amos, L.A., Henderson, R., Unwin, P.N., 1982. Three-dimensional structure determination by electron microscopy of two-dimensional crystals. *Prog. Biophys. Mol. Biol.* 39, 183–231.
- Behlau, M., Mills, D.J., Quader, H., Kühlbrandt, W., Vonck, J., 2001. Projection structure of the monomeric porin OmpG at 6 Å resolution. *J. Mol. Biol.* 305, 71–77.
- Bernal, I., Hamilton, W.C., Ricci, J.S., 1972. *Symmetry: A Stereoscopic Guide for Chemists*. W.H. Freeman and Company, San Francisco, CA, USA.
- Blundell, T.L., Johnson, L.N., 1976. *Protein Crystallography*. Academic Press Inc. (London) Ltd., London, UK.
- Bottcher, B., Wynne, S.A., Crowther, R.A., 1997. Determination of the fold of the core protein of hepatitis B virus by electron microscopy. *Nature* 286, 88–91.
- Caspar, D.L., Klug, A., 1962. Physical principles in the construction of regular viruses. *Cold Spring Harb. Symp. Quant. Biol.* 27, 1–24.
- Crowther, R.A., Henderson, R., Smith, J.M., 1996. MRC image processing programs. *J. Struct. Biol.* 116, 9–16.
- Gipson, B., Zeng, X., Zhang, Z.Y., Stahlberg, H., 2007. 2dx-user-friendly image processing for 2D crystals. *J. Struct. Biol.* 157, 64–72.
- Glaeser, R., 2007. *Electron Crystallography of Biological Macromolecules*. Oxford University Press (USA), New York, NY, USA.
- Glazer, A.M., 1987. *The Structure of Crystals*. IOP Publishing Ltd., Bristol, UK.
- Hahn, T., 2002. *International tables for crystallography Brief Teaching Edition of Volume A: Space-group Symmetry*. Kluwer Academic Publishers, Norwell, MA, USA.

- Hamburger, A.E., West, A.P.J., Hamburger, Z.A., Hamburger, P., Bjorkman, P.J., 2005. Crystal structure of a secreted insect ferritin reveals a symmetric arrangement of heavy and light chains. *J. Mol. Biol.* 349, 558–569.
- Heymann, J.A., Hirai, T., Shi, D., Subramaniam, S., 2003. Projection structure of the bacterial oxalate transporter OxIT at 3.4 Å resolution. *J. Struct. Biol.* 144, 320–326.
- Holser, W.T., 1958. Point groups and plane groups in a two-sided plane and their sub-groups. *Z. Kristallogr* 110, 266–281.
- Kim, K.K., Kim, R., Kim, S.H., 1998. Crystal structure of a small heat-shock protein. *Nature* 394, 595–599.
- Levy, D., Mosser, G., Lambert, O., Moeck, G.S., Bald, D., Rigaud, J.L., 1999. Two-dimensional crystallization on lipid layer: A successful approach for membrane proteins. *J. Struct. Biol.* 127, 44–52.
- Mancini, E.J., Clarke, M., Gowen, B.E., Rutten, T., Fuller, S.D., 2000. Cryo-electron microscopy reveals the functional organization of an enveloped virus, Semliki Forest virus. *Mol. Cell* 5, 255–266.
- Marlovits, T.C., Kubori, T., Sukhan, A., Thomas, D.R., Galan, J.E., Unger, V.M., 2004. Structural insights into the assembly of the type III secretion needle complex. *Science* 306, 1040–1042.
- Mitra, A.K., Yeager, M., van Hoeck, A.N., Wiener, M.C., Verkman, A.S., 1994. Projection structure of the CHIP28 water channel in lipid bilayer membranes at 12-Å resolution. *Biochemistry* 33, 12735–12740.
- Orlova, E.V., Dube, P., Beckman, E., Zemlin, F., Lurz, R., Trautner, T.A., Tavares, P., van Heel, M., 1999. Structure of the 13-fold symmetric portal pore of bacteriophage SPPI. *Nat. Struct. Biol.* 6, 842–846.
- Ranson, N.A., Farr, G.W., Roseman, A.M., Gowen, B., Fenton, W.A., Horwich, A.L., Saibil, H.R., 2001. ATP-bound states of GroEL capture by cryo-electron microscopy. *Cell* 107, 869–879.
- Rhee, K.H., Morris, E.P., Zheleva, D., Hankamer, B., Kühlbrandt, W., Barber, J., 1997. Two-dimensional structure of plant photosystem II at 8-Å resolution. *Nature* 389, 522–526.
- Schenk, A.D., Werten, P.J., Scheuring, S., de Groot, B.L., Muller, S.A., Stahlberg, H., Philippsen, A., Engel, A., 2005. The 4.5 Å structure of human AQP2. *J. Mol. Biol.* 350, 278–289.
- Seelert, H., Poetsch, A., Dencher, N.A., Engel, A., Stahlberg, H., Muller, D.J., 2000. Structural biology. Proton-powered turbine of a plant motor. *Nature* 405, 418–419.
- Senéchal, M., 1990. *Crystalline Symmetries: An Informal Mathematical Introduction*. IOP Publishing Ltd., Bristol, UK.
- Thomas, D.R., Francis, N.R., Xu, C., DeRosier, D.J., 2006. The three-dimensional structure of the flagellar rotor from a clockwise-locked mutant of *Salmonella enterica* serovar Typhimurium. *J. Bacteriol.* 188, 7039–7048.
- Unger, V.M., 2000. Assessment of electron crystallographic data obtained from two-dimensional crystals of biological specimens. *Acta Crystallogr. D* 56, 1259–1269.
- Unger, V.M., Kumar, N.M., Gilula, N.B., Yeager, M., 1997. Projection structure of a gap junction membrane channel at 7 Å resolution. *Nat. Struct. Biol.* 4, 39–43.
- Valpuesta, J.M., Carrascosa, J.L., Henderson, R., 1994. Analysis of electron microscope images and electron diffraction patterns of thin crystals of phi 29 connectors in ice. *J. Mol. Biol.* 240, 281–287.
- Vonck, J., von Nidda, T.K., Meier, T., Matthey, U., Mills, D.J., Kuhlbrandt, W., Dimroth, P., 2002. Molecular architecture of the undecameric rotor of a bacterial Na⁺ATP synthase. *J. Mol. Biol.* 321, 307–316.
- Zhang, X., Shaw, A., Bates, P.A., Newman, R.H., Gowen, B., Orlova, E., Gorman, M.A., Kondo, H., Dokurno, P., Lally, J., Leonard, G., Meyer, H., van Heel, M., Freemont, P.S., 2000. Structure of the AAA ATPase p97. *Mol. Cell* 6, 1473–1484.
- Zhou, Z.H., Baker, M.L., Jiang, W., Dougherty, M., Jakana, J., Dong, G., Lu, G., Chiu, W., 2001. Electron cryomicroscopy and bioinformatics suggest protein fold models for rice dwarf virus. *Nat. Struct. Biol.* 8, 868–873.